ELSEVIER

# The critical role of proximal *gag* sequences in feline immunodeficiency virus genome encapsidation

Iris Kemler, Ishara Azmi, Eric M. Poeschla*

*Molecular Medicine Program, Mayo Clinic College of Medicine, Rochester, MN 55905, USA*

## Abstract

Retroviral RNA encapsidation is mediated by specific interactions between viral Gag proteins and cis-acting packaging sequences in genomic RNA. Feline immunodeficiency virus (FIV) RNA encapsidation determinants have been shown to be discrete and noncontinuous, comprising one region at the 5′ end of the genomic mRNA (R-U5) and another region that mapped within the proximal 311 nt of *gag*. To aid comparative understanding of lentiviral encapsidation and refinement of FIV vector systems, we used RNase protection assays (RPAs) of cellular and virion RNAs to investigate in detail the *gag* element. mRNAs of subgenomic vectors as well as of full-length molecular clones were optimally packaged into viral particles and resulted in high-titer FIV vectors when they contained only the proximal 230 nucleotides (nt) of *gag*. Further 3′ truncations of *gag* sequences progressively diminished encapsidation and transduction. Deletion of the initial ninety 5′ nt of the *gag* gene abolished mRNA packaging, demonstrating that this segment is indispensable for encapsidation. Focusing further on this proximal sequence, we found that a deletion of only 13 nt at the 5′ end of *gag* impaired encapsidation of subgenomic vector and proviral RNAs.
© 2004 Elsevier Inc. All rights reserved.

*Keywords:* Feline immunodeficiency virus (FIV); Human immunodeficiency virus (HIV); Packaging signal; Encapsidation; *gag*; Lentiviral vector

## Introduction

During retroviral assembly, two copies of viral genomic mRNA are incorporated into the nascent viral particle. This process is highly selective in that only unspliced, genomic RNA is encapsidated, whereas spliced (subgenomic) and cellular RNAs are excluded from virions. The specificity of packaging depends on direct binding interactions between the viral Gag polyprotein and cis-acting viral RNA sequences (Berkowitz et al., 1996; Jewell and Mansky, 2000; Lever et al., 1991; Linial and Miller, 1990; Sakalian and Hunter, 1998; Swanstrom and Wills, 1997). In mammalian retroviruses, the RNA sequences that participate in these specific interactions are located in a region that encompasses variable portions of the 5′ untranslated region and usually extend into the proximal *gag* open reading frame (ORF; Linial and Miller, 1990). Because sequences downstream of the major splice donor (MSD) and within *gag* are present

only in the genomic RNA, they contribute to the selective encapsidation of genomic RNA. However, there are reports showing that in simian immunodeficiency virus (SIV), the major packaging determinants are upstream of the MSD (Patel et al., 2003; Strappe et al., 2003). The principal identified packaging determinant in the ASLV group of avian retroviruses is located upstream of the MSD (Banks and Linial, 2000; Katz et al., 1986). Nevertheless, full-length ASLV RNA is highly favored over subgenomic mRNAs for encapsidation, a paradox that remains unexplained (Banks et al., 1998).

In human immunodeficiency virus type 1 (HIV-1) and HIV-2, deletion of the region between the MSD and the *gag* start codon impairs encapsidation and blocks productive replication (Aldovini and Young, 1990; Lever et al., 1989; Poeschla et al., 1998). Four RNA stem-loops that span the MSD (SL1-4) are required for efficient HIV mRNA encapsidation (Berglund et al., 1997; Berkowitz and Goff, 1994; Clever and Parslow, 1997; Harrison and Lever, 1992; Harrison et al., 1998; McBride and Panganiban, 1996, 1997; McBride et al., 1997). RNA mapping experiments suggest that additional encapsidation determinants are present throughout the 5′ end of the mRNA, including U5

---

* Corresponding author. Molecular Medicine, Mayo Clinic College of Medicine, Guggenheim 1811A, 200 First Street SW, Rochester, MN 55905. Fax: +1-507-266-2122.

*E-mail address:* emp@mayo.edu (E.M. Poeschla).

(Helga-Maria et al., 1999; Kaye and Lever, 1999; McBride and Panganiban, 1997; McBride et al., 1997; Vicenzi et al., 1994), a situation that parallels that of feline immunodeficiency virus (FIV) (Kemler et al., 2002). HIV-1 encapsidation determinants are known to extend into *gag* (Buchschacher and Panganiban, 1992; Luban and Goff, 1994; Parolin et al., 1994), and HIV-1 transfer vectors used in gene therapy applications generally contain about 350 nt of *gag* sequences (Dull et al., 1998). Only a few attempts have been made to further characterize the HIV-1 *gag* determinant in direct RNA encapsidation assays (Luban and Goff, 1994; Parolin et al., 1994). These studies suggested that the first 40 nt of *gag* contain elements important for RNA packaging or vector propagation. Nevertheless, HIV-1 *gag* determinants involved in mRNA packaging are not well characterized.

In an initial mapping of FIV encapsidation determinants (Kemler et al., 2002), we found that in contrast to HIV and other mammalian retroviruses, the MSD–*gag* interval contributes negligibly to FIV encapsidation, and deletions in this region did not prevent viral replication. In addition, the 311 proximal nucleotides of FIV *gag* were necessary but not sufficient for encapsidation. This *gag* determinant must clearly be paired with a second determinant upstream of the MSD because deletions there, particularly in U5, markedly reduced encapsidation. No significant encapsidation determinants appear to exist 3′ of *gag* nt 311. Another report is in general agreement with these results (Browning et al., 2003a).

FIV-based lentiviral vectors effectively transduce cells in multiple organ systems (Poeschla, 2003). Development of optimal replication-defective vector systems requires defining the minimum sequences that are necessary and sufficient for RNA encapsidation. This information allows for transfer vector minimization, which reduces risk of replication-competent retrovirus formation. Because the main determinant selecting FIV genomic RNA for packaging over spliced RNA lies within *gag* and because this sequence generates overlap with Gag-encoding sequences in the packaging construct, we decided to further characterize and minimize the encapsidation determinants in the *gag* element. Here we use a competitive encapsidation assay to test subgenomic vectors and proviral clones harboring mutant *gag* sequences for their ability to compete with the full-length wild-type FIV transcripts in RNA packaging, and correlate these data with the transduction efficiencies of the vectors.

## Results and discussion

### The proximal 230 nt of gag are necessary for encapsidation of a subgenomic FIV vector mRNA

We previously demonstrated that *gag* sequences are necessary for encapsidation of FIV subgenomic vectors.

When no *gag* was present, packaging was abolished and marker gene transduction was absent. Inclusion of the proximal 311 nucleotides of *gag* increased encapsidation to nearly wild-type levels and resulted in high titer vectors (Kemler et al., 2002). The mRNA of the vector with 311 nt of *gag* was packaged only slightly less efficiently than the full-length virus transcript (Kemler et al., 2002). To further characterize the proximal *gag* region, we constructed new vectors in which only the length of the proximal *gag* fragment varies (GiNWF-G*n* series, where *n* = no. of *gag* nucleotides). Initially, *gag* was increased from 311 to 350 nt (GiNWF-G350) or decreased to 270 nt (GiNWF-G270), as illustrated in Fig. 1A. To enable robust comparison with our prior data (Kemler et al., 2002), a vector with previously determined encapsidation efficiency (GiNWF-G144) was included in this analysis. The two transfer vectors with the longest *gag* fragments also have a frameshift generated by a single-nucleotide insertion at position 298 of *gag* to prevent expression of potentially interfering Gag protein fragments. Encapsidation efficiencies of mutant mRNAs derived from vectors GiNWF-G0, -G144, -G270, -G311, and -G350 were analyzed in a competitive assay (Kemler et al., 2002) that measures the relative encapsidation efficiencies (REEs) of co-expressed wild-type (CT5efs) and mutant RNAs (GiNWF-G*n*). The benefits of a directly competitive assay are that the same Gag-Pol precursor pools and nascent particles are available to the intracellular viral RNAs and that analysis of both RNAs within the same cellular and virion samples obviates problems with intersample variations accrued incrementally during transfection, RNA recovery, and RPAs (McBride and Panganiban, 1996). CT5efs is a full-length proviral clone with a 29 nt *env*-frameshifting ("efs") oligonucleotide insertion in the SU domain. It was used rather than CT5 to generate the wild-type mRNA to eliminate FIV Env-induced cell lysis, which is prominent in 293T cells via CXCR4-induced fusion (Poeschla and Looney, 1998), and which could contaminate virion pellets with intracellular RNA. CT5efs provides all virion proteins necessary for packaging of its own mRNA and of the subgenomic vector mRNAs. Cellular RNA and RNA from virion particles pelleted through sucrose cushions were isolated. Virion RNA was extracted from equivalent amounts of viral particles, as determined by RT assay. RNAs were then subjected to an RNase protection assay (RPA) with a ^{32}P-labeled riboprobe that distinguishes between the wild-type (CT5efs) and mutant (GiNWF-G*n*) RNAs. The REE of the mutant was determined by calculating the ratio of mutant RNA to wild-type RNA in the virion, relative to the ratio of the two RNAs in the cytoplasm (Kemler et al., 2002; McBride et al., 1997). Each virion RNA was analyzed in two different amounts (1× and 3×). The calculated REEs in each figure correspond to the particular experiment shown in the figures. A summary of mean REEs derived from multiple experiments is shown in Table 1. CT5efs and the *gag*-variant vector plasmids transcribed
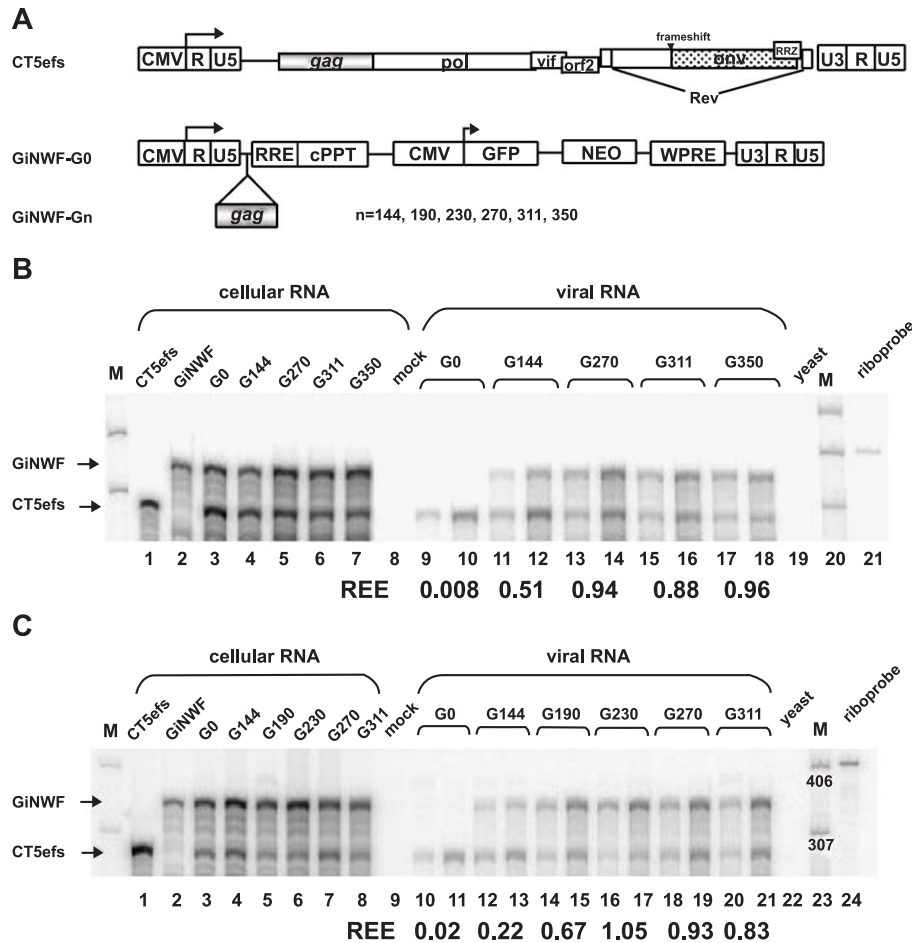
Fig. 1. The proximal 230 nt of *gag* are necessary for efficient encapsidation of FIV subgenomic RNAs. (A) Schematic representation of pCT5efs and pGiNWF-G*n* constructs. (B) RPA of a competitive encapsidation experiment in which wild-type CT5efs was cotransfected with GiNWF-G0, -G144, -G270, -G311, or -G350 into 293T cells. Cellular RNA and viral RNA were subjected to an RPA with a $^{32}$P-labeled riboprobe complementary to the central DNA flap region (pSPT-FLAP). Protected RNA species are 358 nt for all GiNWF-G*n* constructs and 296 nt for CT5efs. (C) RPA of a competitive encapsidation experiment in which wild-type CT5efs was cotransfected with GiNWF-G0, -G144, -G190, -G230, -G270, -G311 into 293T cells. Riboprobe pSPT-FLAP was used. Relative encapsidation efficiency (REE) was determined by calculating the ratio of mutant RNA to wild-type RNA in the virion, relative to the ratio in the two RNAs in the cytoplasm (Kemler et al., 2002).

similar amounts of RNA (Fig. 1B, cellular RNA, compare upper and lower bands in lanes 3–7). Consistent with previous data (Kemler et al., 2002), when no *gag* sequences were present in the vector (GiNWF-G0), RNA packaging was abolished (Fig. 1B, lanes 9 and 10). There was little difference observed between vectors having 270 nt of *gag* (REE = 0.94; lanes 13 and 14), 311 nt of *gag* (REE = 0.88; lanes 15 and 16), or 350 nt of *gag* (REE = 0.96; lanes 17 and 18).

The finding that 270 nt of *gag* sequences conferred an REE of 0.94 prompted study of additional truncations. GiNWF-G230 and GiNWF-G190 have 230 and 190 nt, respectively, of *gag* sequence (Fig. 1A). As shown in Fig. 1C, a transfer vector with 230 nt of *gag* is optimal, resulting in an REE of 1.05 (lanes 16 and 17). Further deletion of *gag* sequences to 190 nt reduced packaging to a REE of 0.67 (lanes 14 and 15). As previously seen (Kemler et al., 2002), a vector with only 144 nt of *gag* sequences was further

impaired in mRNA packaging (Fig. 1B, lanes 11 and 12; Fig. 1C, lanes 12 and 13). These results clearly identify nucleotide 230 as the right-hand boundary of *gag* sequences necessary for optimal encapsidation.

To determine whether the length of the *gag* fragment has a corresponding effect on vector transduction efficiencies, CrFK cells were infected with RT-normalized viral stocks of VSV-G-pseudotyped vectors GiNWF-G0, -G144, -G190, -G230, -G270, -G311, and the number of GFP-expressing cells was determined by FACS analysis (Fig. 2). GiNWF-G230 had a transduction efficiency of $2.37 \times 10^6$ TU/ml $\pm$ $1.76 \times 10^5$ exceeding GiNWF-G311 ($1.22 \times 10^6$ TU/ml $\pm$ $1.71 \times 10^5$) and -G270 ($1.61 \times 10^6$ TU/ml $\pm 1.76 \times 10^5$). As expected, GiNWF-G0 transduced very poorly. The GiNWF-G144 vector nevertheless appreciably transduces, although with a lower efficiency. Thus, the encapsidation efficiencies and transduction efficiencies of the subgenomic vectors correlate very well.

Table 1
Relative encapsidation efficiencies

| Vector | REE | Provirus | REE |
|---|---|---|---|
| GiNWF-GO | 0.03 ± 0.01 | CT5-G0 | 0.10 ± 0.06 |
| GiNWF-G144 | 0.28 ± 0.15 | CT5-G144 | 0.20 |
| GiNWF-G190 | 0.67 | CT5-G190 | 0.64 |
| GiNWF-G230 | 1.24 ± 0.27 | CT5-G230 | 0.95 ± 0.03 |
| GiNWF-G270 | 0.94 ± 0.01 | CT5-G270 | 0.75 |
| GiNWF-G311 | 0.86 ± 0.02 | | |
| GiNWF-G350 | 0.96 | CT5-G350 | 0.78 |
| GiNWF-G45-230 | 0.20 ± 0.14 | CT5-G45-230 | 0.16 ± 0.05 |
| GiNWF-G34-230 | 0.17 ± 0.04 | CT5-G34-230 | 0.20 ± 0.02 |
| GiNWF-G23-230 | 0.28 ± 0.00 | | |
| GiNWF-G13-230 | 0.37 ± 0.02 | CT5-G13-230 | 0.52 |

The relative encapsidation efficiencies (REE) of the mutant vector or proviral RNAs were determined by calculating the ratio of mutant RNA to wild-type RNA in the virion, relative to the ratio of the two RNAs in the cytoplasm. Calculations of standard deviations are based on results of two to four independent experiments.

## The proximal 230 nt of gag are essential for efficient packaging of a genomic proviral RNA

In the GiNWF-G*n* subgenomic vectors, the *gag* fragment is followed by the Rev-responsive element (RRE), a juxtaposition that could influence encapsidation by resulting in artificial secondary structures. Therefore, here and elsewhere in these studies, we tested our conclusions about the *gag* sequences in a second context: full-length proviruses in which only the *gag* fragment was altered (Fig. 3A). The packaging efficiencies of the mutant CT5-G*n* proviruses were analyzed in a competitive assay with the wild-type CT5efs provirus. The mutant proviruses showed REEs similar to those of corresponding mutant subgenomic vectors (compare Fig. 3B with Figs. 1B and C). Absence of *gag* sequences in the provirus completely abolished encapsidation (REE 0.07, Fig. 3B, lanes 9 and 10), whereas inclusion of the first 230 nt of *gag* resulted in the highest mRNA packaging (REE 0.95, lanes 14 and 15). Longer *gag* fragments (CT5-G270, CT5-G350) as well as shorter *gag* fragments (CT5-G190, CT5-G144) had a negative influence on mRNA encapsidation. These data (Figs. 1 and 3), in which firm agreement was observed in both the full-length virus and subgenomic vector contexts, establish definitively the presence of an important packaging determinant in the first 230 nt of the FIV *gag* gene.

Our results disagree with Browning et al. (2003b), who concluded that 100 bp of *gag* in conjunction with the 5′ UTR are sufficient for efficient FIV RNA encapsidation, and that RNA is detectably packaged even in the absence of any *gag*. Important methodological differences include the use of the slot blot technique in the latter study to measure RNAs, which does not confine measurements to single size-specific bands as in the preferable RPAs used in our study. In addition, the experimental design was a noncompetitive encapsidation assay, where wild-type and mutant RNAs are expressed in separate transfections (Browning et al., 2003b). In contrast, we used a directly competitive encapsidation assay, which measures the relative encapsidation efficiencies of wild-type and mutant RNAs co-expressed within the same cell (Kemler et al., 2002; McBride and Panganiban, 1996).

## Short deletions at the 5′ end of the FIV gag gene drastically impair FIV RNA encapsidation

We established previously that in FIV deletions between the major SD and the *gag*, ATG start did not significantly attenuate encapsidation (Kemler et al., 2002). Having now further mapped the 3′ boundary of the *gag* determinant to nt 230 with the 3′ to 5′ truncations, we used 5′ to 3′ *gag* deletions to determine whether sequences in the 5′ proximal *gag* gene contributed to RNA packaging. New subgenomic vectors containing incremental forward 5′→3′ deletions starting at the *gag* ATG were made (GiNWF-G45-230, -G90-230, -G135-230, -G180-230, Fig. 4A). Testing of the three vectors with the longest deletions, GiNWF-G90-230 (Fig. 4B, lanes 6 and 7), -G135-230, and -G180-230 (data not shown) showed that mRNA encapsidation was completely abolished, comparable to GiNWF-G0. Only GiNWF-G45-230 resulted in appreciable mRNA packaging (REE 0.12, lanes 4 and 5). Similar results were obtained when these *gag* mutants were placed in the context of a provirus (data not shown). Genomic RNA from proviral clones CT5-G90efs, CT5-G135efs, and CT5-G0efs was absent from viral particles. In contrast, CT5-G45-230efs-derived RNA was encapsidated with a REE of 0.18 (Fig. 4C, lanes 10 and 11). These results show that the first 90 nt of *gag* contain an absolutely essential encapsidation determinant. However, the results did not clearly define a left-hand boundary of packaging determinants in *gag* because the GiNWF-G45-230 subgenomic vector and the corresponding proviral clone CT5-G45-230 showed a fivefold lower encapsidation efficiency than the wild-type provirus CT5efs. Therefore, more precise deletions were made at the 5′ end of *gag*, with the shortest
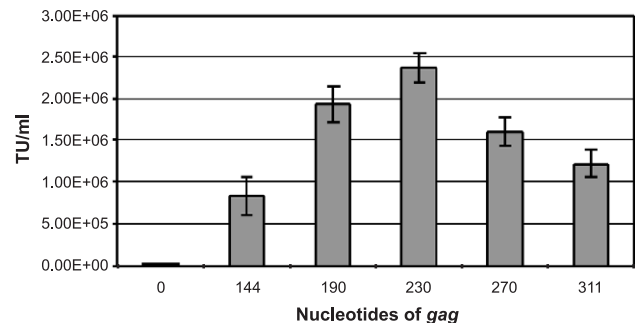


Fig. 2. Infectivity determinations for FIV vectors with different lengths of *gag* fragment. CrFK cells were infected with RT activity-normalized viral stocks of VSV-G pseudotyped vectors GiNWF-G0, -G144, -G190, -G230, -G270, -G311. GFP-expressing cells were analyzed by FACS (Loewen et al., 2003) and titers were expressed as the mean ± SD of four independent experiments.
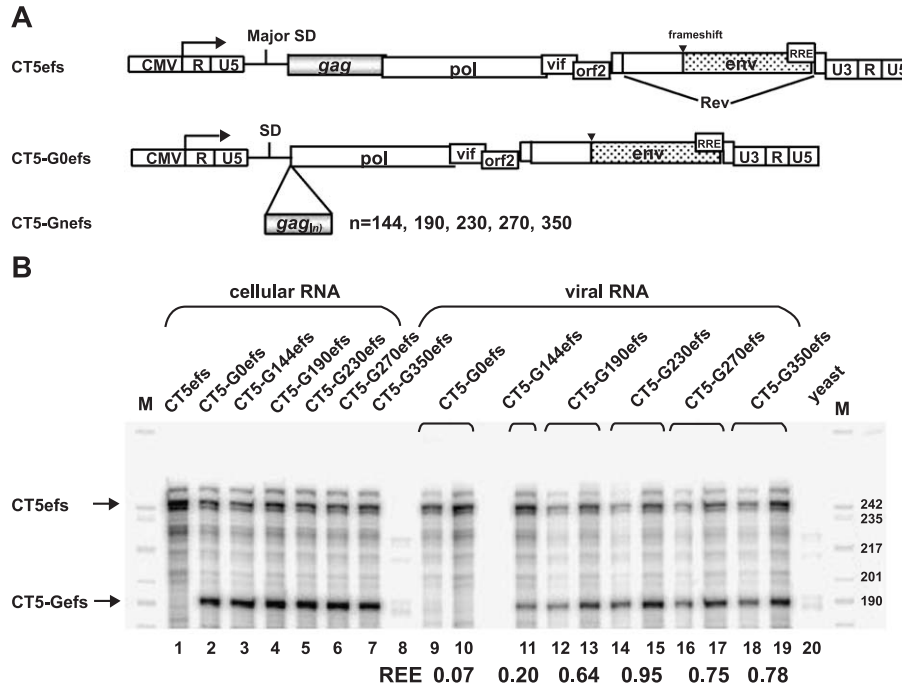
Fig. 3. The proximal 230 nt of *gag* are necessary for efficient encapsidation of FIV proviral clones. (A) Schematic representation of CT5efs and CT5-Gefs clones, proviral clones with either all of *gag* deleted (CT5-G0efs) or with increasing amounts of *gag* (CT5-G144efs, -G190efs, -G230efs, -G350efs). (B) RPA of a competitive encapsidation experiment. Wild-type CT5efs was cotransfected with the CT5-Gefs mutants into 293T cells. Cellular RNA and viral RNA were subjected to an RPA with a $^{32}$P-labeled riboprobe complementary to genome nucleotides 1847–2094 (pSPT-CT5MP). Protected RNA species are 247 nt for CT5efs and 193 nt for CT5-Gefs clones. Relative encapsidation efficiencies are indicated at the bottom.

deleting as few as 13 nt (GiNWF-G13-230, -G23-230, -G34-230, Fig. 4A). Reducing further the degree of truncation at the 5′ end by incrementally restoring *gag* sequences improved encapsidation of the vector mRNA (Fig. 4B) as well as their corresponding proviral RNAs (Fig. 4C). The mutants with either 45 or 34 nt of *gag* sequence deleted showed comparable relative encapsidation efficiencies (GiNWF-G45-230: 0.09, GiNWF-G34-230: 0.14, Fig. 4B, lanes 21–24; and CT5-G45-230efs: 0.18, CT5-G34-230efs: 0.18, Fig. 4C, lanes 10–13). Inclusion of an additional 11 nt, GiNWF-G23-230, further increased packaging to 0.28 (Fig. 4B, lanes 25 and 26). Surprisingly, restoration of 10 more nucleotides to GiNWF-G23-230, resulting in GiNWF-G13-230 (a vector with only the 13 most 5′ nt of *gag* deleted), reduced RNA encapsidation threefold compared to wild-type (REE = 0.35, Fig. 4B, lanes 27 and 28). Similarly, packaging of the corresponding proviral RNA CT5-G13-230efs was reduced twofold (Fig. 4C, lanes 14 and 15). These results suggest that the most proximal 5′ end of *gag* contributes significantly to FIV mRNA packaging.

All the mutant subgenomic vectors (GiNWF-G) and the corresponding proviral clones (CT5-G) harboring 5′ →3′ deletions in *gag* analyzed so far (Fig. 4) contain a *gag* gene truncated at position 230. In order to rigorously test the contribution of proximal *gag* sequences in FIV mRNA encapsidation, we next tested full-length proviral clones having only 13 nt (CT5Δ13), 23 nt (CT5Δ23) or 90 nt

(CT5Δ90) deleted at the 5′ end of *gag* (Fig. 5A). These clones were otherwise identical to the wild-type provirus CT5efs. Cellular and viral RNAs were analyzed with a riboprobe that spans the major splice donor and therefore detects both unspliced genomic and spliced subgenomic RNAs. Genomic mRNA with a 13 nt (CT5Δ13) or 23 nt (CT5Δ23) deletion at the 5′ end was packaged twofold less efficiently than the wild-type CT5efs genomic RNA (Fig. 5B, lanes 7–10). In CT5Δ90, which has the first 90 nt of the *gag* ORF deleted, a dramatic reduction in packaging was observed with an REE of 0.17 (lanes 11 and 12). Thus, the 5′ end of *gag*, particularly the first 90 nt, contains an indispensable determinant for mRNA encapsidation. This element tolerates little alteration because a deletion as small as 13 nt (GiNWF-G13-230, CT5-G13-230efs, CT5Δ13) has a strong effect on packaging. These experiments establish a strong left-hand boundary of the *gag* determinant.

This *gag* determinant might promote folding of RNA secondary structure favorable for either Gag polyprotein recognition or RNA dimerization. It is also possible that *gag* sequences are part of a bipartite RNA packaging signal that includes leader sequences such as R or U5, which we previously have shown to be important for RNA packaging. The *gag* determinant is necessary but not sufficient for packaging because vector RNAs lacking leader sequences are not encapsidated (Kemler et al., 2002). In HIV-1, a novel RNA conformation was recently found that contains a long
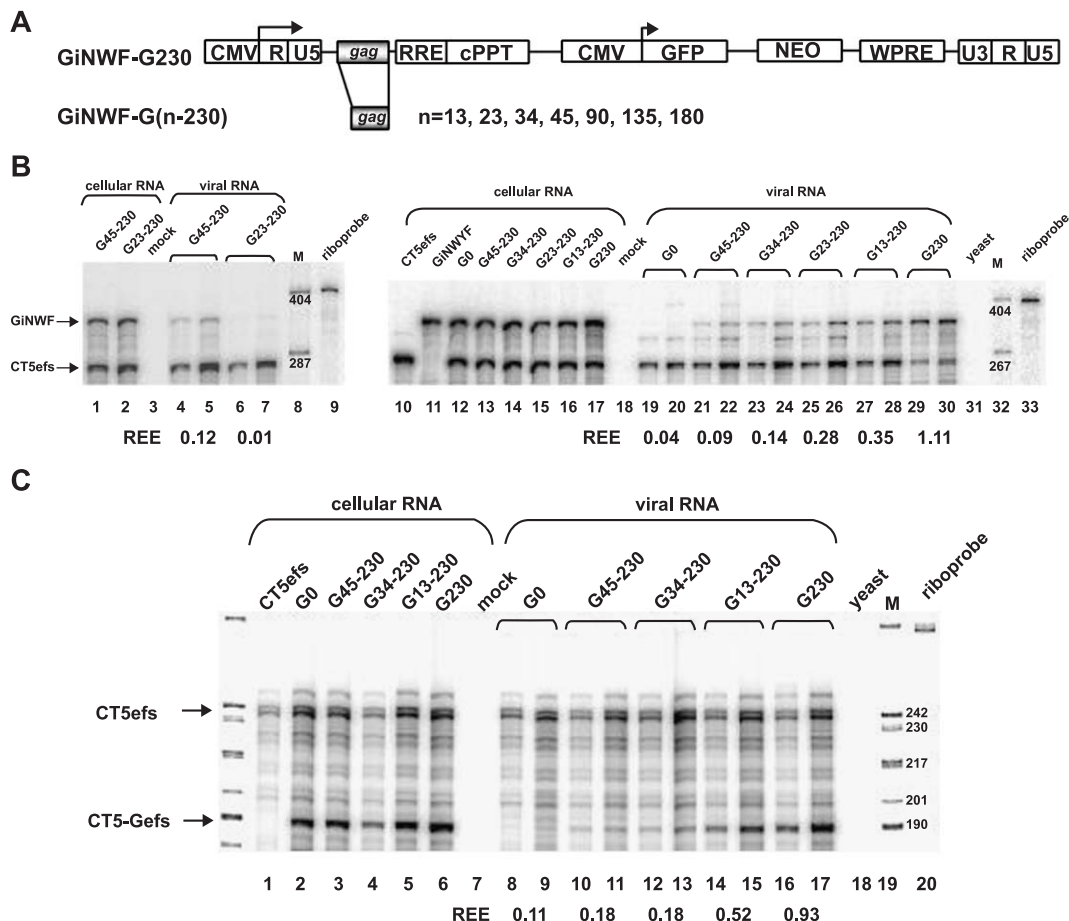
Fig. 4. Requirement of the proximal 90 nt of FIV *gag* for encapsidation. (A) Schematic representation of GiNWF-G*n* clones. Subgenomic FIV transfer vector GiNWF-G230 was used to introduce increasing deletions beginning at the *gag* ATG start codon. (B) RPA of a competitive encapsidation experiment. Wild-type CT5efs was cotransfected with GiNWF-G45-230 and GiNWF-G90-230 (lanes 1–7) or with GiNWF-G0, -G45-230, G34-230, G23-230, G13-230, -G0 (lanes 12–30) into 293T cells. Cellular RNA and viral RNA were subjected to an RPA with a $^{32}$P-labeled riboprobe complementary to the central DNA flap (pSPT-FLAP). Protected RNA species are 358 nt for all GiNWF-G clones and 296 nt for CT5efs. (C) RPA of a competitive encapsidation experiment. Wild-type CT5efs was cotransfected with CT5-G0efs, -G45-230efs, -G90-230efs, -G135-230efs, -G230efs into 293T cells. Cellular RNA and viral RNA were subjected to an RPA with a $^{32}$P-labeled riboprobe complementary to genome nucleotides 1847–2094 (pSPT-CT5MP). Protected RNA species are 247 nt for CT5efs and 193 nt for CT5-Gefs clones.

distance base-pairing interaction between U5 sequences and sequences including the *gag* initiation codon (Abbink and Berkhout, 2003).

The proximal 90 nt of *gag* might facilitate interactions of viral RNA with Gag polyproteins involved in particle formation by adopting a specific RNA secondary structure. Recombinant HIV-1 Gag polyprotein shows strong in vitro binding to the proximal 170 nt of *gag* measured by RNA gel mobility shift assays (Berkowitz et al., 1993; Luban and Goff, 1991). Binding is most probably mediated by RNA secondary structure, similarly to binding of nucleocapsid (NC) to the stem-loop structure SL3 in the HIV leader (De Guzman et al., 1998).

Whether packaging and dimerization are clearly linked processes has been controversial (Swanstrom and Wills, 1997). One model of HIV-1 dimerization involves a "kissing-loop" mechanism and proposes that RNA dimerization is initiated by the SL1 loop palindrome sequence

via the formation of regular Watson–Crick base pairs. In FIV, however, an analogous kissing-loop mechanism has not been found, nor does modeling of RNA secondary structures reveal a stem-loop structure containing a palindromic loop. A second dimerization model for HIV-1 suggests that a tetra-stranded RNA structure, formed by G-rich RNA sequences, results in RNA dimerization. In vitro dimerization studies showed that guanine tracts in HIV-1 *gag* were required for dimerization (Awang and Sen, 1993; Haddrick et al., 1996; Sundquist and Heaphy, 1993), although later evidence suggested that the G-quartets are not required in vivo for dimerization or packaging (Haddrick et al., 1996; Russell et al., 2003). In FIV, two G-rich elements with potential to form quartets can be found in proximal *gag*. The first element is from nucleotides 3 to 6 of *gag* and the second is found at position 70 to 75. As the first 90 nucleotides of *gag* contain a determinant absolutely required for RNA encapsidation,
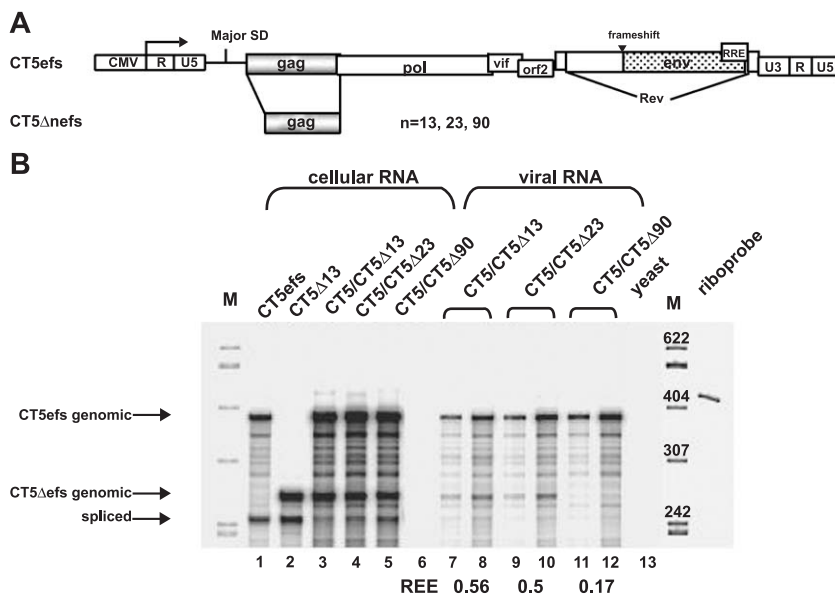
Fig. 5. Contribution of proximal *gag* sequences to encapsidation of full-length viral genomic mRNAs. (A) Schematic representation of CT5efs, CT5Δ13efs, CT5Δ23efs, and CT5Δ90efs. (B) RPA of a competitive encapsidation experiment. Wild-type CT5efs was cotransfected with CT5Δ13, CT5Δ23, or CT5Δ90 into 293T cells. Cellular and virion RNAs were subjected to an RPA with a $^{32}$P-labeled riboprobe complementary to genome nucleotides 359–740 (pSPT-CT5BN). Lengths of protected fragments are CT5efs genomic RNA 382 nt, CT5Δ13, CT5Δ23, CT5Δ90 genomic RNA 266 nt, all spliced RNAs 244 nt. Lane 6, mock-transfected cells.

the possibility exists that this region is also involved in FIV RNA dimerization and encapsidation through the formation of G-quartets.

The present results are the most detailed analysis yet of *gag* packaging determinants in a lentivirus. Maintenance of 350 or more nt of *gag* in HIV-1 transfer vectors has been effective in gene therapy applications (Dull et al., 1998), but the basis for the requirement has not been well investigated. Although RNA stem-loops SL1 to SL4 in HIV-1 have been examined in many encapsidation analyses, surprisingly few studies (Buchschacher and Panganiban, 1992; Luban and Goff, 1994; Parolin et al., 1994) have characterized the HIV-1 *gag* determinant. Luban and Goff (1994) showed that an RNA lacking the first 40 nt of the *gag* coding sequence had a greatly impaired capacity of RNA packaging. However, a minimal *gag* sequence requirement for packaging or transduction was not defined. In another report, titers of HIV transfer vectors encoding a selectable marker gene having 53 or 722 bp of *gag* were analyzed. The vector with 722 nt of *gag* sequence produced moderately higher titers in this system, but packaging of those vector RNAs was not examined (Buchschacher and Panganiban, 1992). The third of these studies found that inclusion of 40 or 653 nt of *gag* sequence in the vector increased the efficiency of gene transfer by 16- and 32-fold, respectively (Parolin et al., 1994). This increase was partly due to increased packaging of vector RNA.

It is clear from the present data that deletions close to the 5′ end of FIV *gag* have a strong negative influence on FIV genome RNA encapsidation. Inclusion of the proximal 230

nt of *gag* is optimal for genomic RNA packaging and transduction efficiency of a FIV vector. Establishing a right-hand boundary for this element will optimize FIV-based lentiviral vectors. The 230 nt of *gag* are the only sequences remaining in overlap with the packaging plasmid, and this overlap can eventually be eliminated by synonymous nucleotide changes in *gag*.

## Materials and methods

### Plasmid construction

Numbering of nucleotides follows Talbott et al. (1989). All mutants were confirmed by automated DNA sequencing. pCT5efs is a variant of wild-type FIV expression construct pCT5 (Poeschla and Looney, 1998; Poeschla et al., 1998) with an *env* frame-shifting (efs) oligonucleotide insertion (29 bp) in the SU domain at nt 7176. GiNWF-G*n* constructs are FIV vector plasmids that contain, from 5′ to 3′, the hybrid U3-substituted promoter of pCT5, R, U5, leader sequence, varying amounts of *gag* sequence (*n* = no. of *gag* nucleotides), the Rev response element (RRE), a sequence containing the FIV central polypurine tract (cPPT) and the central termination sequence (CTS) (Whitwam et al., 2001), the human CMV immediate early promoter, *egfp*, an internal ribosomal entry site (IRES), neoR, the woodchuck hepatitis virus post-transcriptional regulatory element (WPRE), and the 3′ long terminal repeat (LTR). The cPPT-CTS combination is also referred to as the central DNA flap, as the strand initiations and terminations

that occur at these loci result in a triple-stranded DNA flap structure at the completion of FIV reverse transcription. GiNWF-G0, GiNWF-G144, GiNWF-G311, and GiNWF-G407 were described previously (Kemler et al., 2002). The other GiNWF-G constructs were generated by PCR with the sense primer FIV11842 (5′-GCTTAGGGTTAGGCG-TTTTGCGCTGC-3′) and one of the following SphI-tailed antisense primers: FIV818-SphAS (5′-ATATGCATGCG-TACTAACCAACCTTAGTTGATC-3′) for GiNWF-G190, FIV858-SphAS (5′-ATATGCATGCGTACGCTAGATC-CAAATTTTTCTC-3′) for GiNWF-G230, FIV 898-SphAS (5′-ATATGCATGCGTACCAAAGACTTTTAATGTCAC-3′) for GiNWF-G270, FIV978-SphAS (5′-ATATG-CATGCGTACAGTGTCTAATCCCATTTGAG-3′) for GiNWF-G350. The PCR products were restricted with MluI and SphI and ligated to the 7208 bp MluI−SphI backbone of GiNWF-G313. All plasmids were sequenced.

GiNWF-G clones containing incremental 5′ → 3′ deletions in gag were generated by PCR with the antisense primer FIV858SphAS (5′-ATATGCATGCGTACGCTA-GATCCAAATTTTTCTC-3′) and one of the following sense primers: FIV-Nla640 (5′-ATATCATGCAGGGGC-GAGATTGGAAAATG-3′) for GiNWF-G13-230, FIV-Nla650 (5′-ATATCATGATTGGAAAATGGCCATTAAG-3′) for GiNWF-G23-230, FIV-Nla661 (5′-ATATCATGGC-CATTAAGAGATGTAG-3′) for GiNWF-G34-230, FIV-Nla672 (5′-ATATCATGATGTAGTAATGTTGCTGTAGG-3′) for GiNWF-G45-230, FIV-Nla717 (5′-ATATCATGTG-GAGAAGGGAATTTCAG-3′) for GiNWF-G90-230, FIV-Nla762 (5′-ATATCATGTACAGGACGAGAACCTGG-3′) for GiNWF-G135-230, FIV-Nla858 (5′-ATATCAT-GAAGGTTGGTTATTTGCG) for GiNWF-G180-230. GiNWF-G230 was used as a template. PCR fragments were restricted with NlaIII, blunted and restricted with SphI. Fragments were cloned into GiNWF-G0 between position 627 (BsiWI site blunted) and position 632 (Sph site). All plasmids were sequenced. CT5-G13-230efs was constructed by isolating a 3656 bp SphI (blunted)−NotI fragment from GiNWF-G13-230 and ligating it to a 7574 bp PstI (blunted)−NotI fragment derived from CT5efs. The other CT5-Gefs clones were made correspondingly.

CT5Δ13 was constructed by inserting a 1117 bp MluI−BstXI from GiNWF-G13-230 into CT5efs restricted with MluI and EcoRI (10 019 bp) together with an 875 bp BspMI−EcoRI fragment from CT5efs and a 258 bp BstXI−BspMI fragment from GiNWF-G1226, containing a frameshifting mutation at position 298 of gag to prevent expression of potentially interfering Gag protein fragments. CT5Δ23 and CT5Δ90 were made correspondingly. All plasmids were sequenced.

Plasmids used as templates for production of riboprobes were constructed as follows. pSPT-CT5MP was generated by inserting a 247 bp PflMI−MseI fragment from position 1847 to 2094 of CT5efs into pSPT18 (Roche) digested with SmaI. The resulting plasmid was linearized with SacI. The protected RNA species are 247 nt for CT5efs and 193

nt for CT5-Gefs clones. pSPT-CT5BN was generated by inserting a 382 bp NarI−BstXI fragment from position 359 to 740 of CT5efs into pSPT19 (Roche) digested with SmaI and AccI. The resulting plasmid was linearized with HindIII. The protected RNA species are 382 nt for CT5 genomic RNA, 266 and 103 nt for CT5Δ13 genomic RNA, 266 and 93 nt for CT5Δ23 genomic RNA, 266 nt for CT5Δ90 genomic RNA, and 244 nt for all spliced RNAs. pSPT-FLAP was described in Kemler et al. (2002). Protected RNA species are 358 nt for all GiNWF-G clones and 296 nt for CT5efs.

## Cell culture and transfections

293T and Crandell feline kidney (CrFK) cells were cultured in Dulbecco's modified Eagle medium with 10% fetal calf serum. Transient transfections were performed by the calcium phosphate coprecipitation method. In competitive encapsidation assays, 7.5 μg of pCT5efs (wild-type) and 7.5 μg of mutant plasmid were cotransfected.

## RNA isolation

Forty-two hours after transfection cellular RNA was isolated with Trizol (Invitrogen) according to the manufacturer's protocol. Viral particles were purified from the medium by removing cell debris by centrifugation at $828 \times g$ in a Sorvall table top centrifuge for 10 min and filtering the clarified supernatant through a 0.45 μm filter. The virus was then pelleted through a 20% sucrose cushion for 2 h at $112 700 \times g$ in a SW28 rotor. The viral pellet was resuspended in TNE buffer (10 mM Tris, pH 7.5, 100 mM NaCl, 1 mM EDTA) and aliquots were stored at $-80$ °C. Viral particle production was measured by a reverse transcriptase assay. Viral RNA was isolated by disrupting the particles in 1% SDS, proteinase K (100 μg/ml) at 37 °C for 30 min in the presence of 10 μg yeast RNA. After two extractions with phenol (pH 4.5)−chloroform, RNA was ethanol precipitated in the presence of 0.3 M sodium acetate. Both cellular and viral RNAs were treated with 10U RNase-free DNase I in a buffer containing 20 mM Tris, pH 8.0, 10 mM MgCl$_2$, and 40U RNase inhibitor (Roche) at 37 °C for 30 min. The reaction was terminated by adding an equal volume of a $2\times$ stop buffer (0.4% SDS, 0.6 M sodium acetate, 20 mM EDTA). The RNA was extracted with phenol−chloroform and precipitated with ethanol. The concentration of cellular RNA was determined by measuring the spectrophotometric absorption at 260 nm.

## RNase protection assay

$^{32}$P-labeled riboprobes were synthesized by in vitro transcription of linearized plasmids, using SP6 RNA polymerase (Roche), $\alpha^{32}$P-rUTP (800 Ci/mmol), and 5 μM unlabeled rUTP. Riboprobes were purified from 6% polyacrylamide-8 M urea gels before use. The RPA was

performed with a commercially available kit (Ambion) according to the manufacturer's protocol. Five micrograms of cellular RNA or different amounts of viral RNA supplemented with 2 µg yeast RNA was mixed with $5 \times 10^5$ cpm of $^{32}$P-labeled probe in 10 µl hybridization buffer and incubated at 42 °C for 12 h. Unhybridized regions were then digested with 0.37U RNase A and 15U RNase T1 for 30 min at 37 °C. Protected fragments were precipitated, resuspended in RNA loading buffer, and separated on 6% polyacrylamide–8 M urea gels. For size determination, $\alpha^{32}$P-dCTP labeled fragments of pBR322 digested with MspI were run in parallel. Protected RNA species were quantified by PhosphorImager analysis (Molecular Dynamics).

## Vector transduction efficiencies and RT assay

VSV-G pseudotyped vectors were produced in 293T cells by transfecting 3 µg of GiNWF-G plasmid together with 1 µg pMD.G (VSV-G) and 3 µg FP93 (packaging plasmid, provides Gag/Pol proteins, lacks all viral sequences upstream of gag; Loewen et al., 2003). Transduction efficiencies were determined as described by Loewen et al. (2003). CrFK cells were infected with 10-fold serial dilutions of RT-normalized VSV-G pseudotyped GiNWF-G vectors. Forty-eight hours later, cells were trypsinized, fixed in 1% formalin–PBS, and analyzed for GFP-expressing cells by fluorescence-activated flow cytometry (FACS). The RT assay was performed as described in Kemler et al. (2002).

## Acknowledgments

## References

Abbink, T.E., Berkhout, B., 2003. A novel long distance base-pairing interaction in human immunodeficiency virus type 1 RNA occludes the Gag start codon. J. Biol. Chem. 278 (13), 11601–11611.

Aldovini, A., Young, R.A., 1990. Mutations of RNA and protein sequences involved in human immunodeficiency virus type 1 packaging result in production of noninfectious virus. J. Virol. 64 (5), 1920–1926.

Awang, G., Sen, D., 1993. Mode of dimerization of HIV-1 genomic RNA. Biochemistry 32 (42), 11453–11457.

Banks, J.D., Linial, M.L., 2000. Secondary structure analysis of a minimal avian leukosis-sarcoma virus packaging signal. J. Virol. 74 (1), 456–464.

Banks, J.D., Yeo, A., Green, K., Cepeda, F., Linial, M.L., 1998. A minimal avian retroviral packaging sequence has a complex structure. J. Virol. 72 (7), 6190–6194.

Berglund, J.A., Charpentier, B., Rosbash, M., 1997. A high affinity binding site for the HIV-1 nucleocapsid protein. Nucleic Acids Res. 25 (5), 1042–1049.

Berkowitz, R.D., Goff, S.P., 1994. Analysis of binding elements in the human immunodeficiency virus type 1 genomic RNA and nucleocapsid protein. Virology 202 (1), 233–246.

Berkowitz, R.D., Luban, J., Goff, S.P., 1993. Specific binding of human immunodeficiency virus type 1 gag polyprotein and nucleocapsid protein to viral RNAs detected by RNA mobility shift assays. J. Virol. 67 (12), 7190–7200.

Berkowitz, R., Fisher, J., Goff, S.P., 1996. RNA packaging. Curr. Top. Microbiol. Immunol. 214 (4), 177–218.

Browning, M.T., Mustafa, F., Schmidt, R.D., Lew, K.A., Rizvi, T.A., 2003a. Delineation of sequences important for efficient packaging of feline immunodeficiency virus RNA. J. Gen. Virol. 84 (Pt 3), 621–627.

Browning, M.T., Mustafa, F., Schmidt, R.D., Lew, K.A., Rizvi, T.A., 2003b. Sequences within the gag gene of feline immunodeficiency virus (FIV) are important for efficient RNA encapsidation. Virus Res. 93 (2), 199–209.

Buchschacher Jr., G.L., Panganiban, A.T., 1992. Human immunodeficiency virus vectors for inducible expression of foreign genes. J. Virol. 66 (5), 2731–2739.

Clever, J.L., Parslow, T.G., 1997. Mutant human immunodeficiency virus type 1 genomes with defects in RNA dimerization or encapsidation. J. Virol. 71 (5), 3407–3414.

De Guzman, R.N., Wu, Z.R., Stalling, C.C., Pappalardo, L., Borer, P.N., Summers, M.F., 1998. Structure of the HIV-1 nucleocapsid protein bound to the SL3 psi-RNA recognition element. Science 279 (5349), 384–388.

Dull, T., Zufferey, R., Kelly, M., Mandel, R.J., Nguyen, M., Trono, D., Naldini, L., 1998. A third-generation lentivirus vector with a conditional packaging system. J. Virol. 72 (11), 8463–8471.

Haddrick, M., Lear, A.L., Cann, A.J., Heaphy, S., 1996. Evidence that a kissing loop structure facilitates genomic RNA dimerisation in HIV-1. J. Mol. Biol. 259 (1), 58–68.

Harrison, G.P., Lever, A.M., 1992. The human immunodeficiency virus type 1 packaging signal and major splice donor region have a conserved stable secondary structure. J. Virol. 66 (7), 4144–4153.

Harrison, G.P., Miele, G., Hunter, E., Lever, A.M., 1998. Functional analysis of the core human immunodeficiency virus type 1 packaging signal in a permissive cell line. J. Virol. 72 (7), 5886–5896.

Helga-Maria, C., Hammarskjold, M.L., Rekosh, D., 1999. An intact TAR element and cytoplasmic localization are necessary for efficient packaging of human immunodeficiency virus type 1 genomic RNA. J. Virol. 73 (5), 4127–4135.

Jewell, N.A., Mansky, L.M., 2000. In the beginning: genome recognition, RNA encapsidation and the initiation of complex retrovirus assembly. J. Gen. Virol. 81 (Pt 8), 1889–1899.

Katz, R.A., Cullen, B.R., Malavarca, R., Skalka, A.M., 1986. Role of the avian retrovirus mRNA leader in expression: evidence for novel translational control. Mol. Cell. Biol. 6 (2), 372–379.

Kaye, J.F., Lever, A.M., 1999. Human immunodeficiency virus types 1 and 2 differ in the predominant mechanism used for selection of genomic RNA for encapsidation. J. Virol. 73 (4), 3023–3031.

Kemler, I., Barraza, R., Poeschla, E.M., 2002. Mapping of the encapsidation determinants of feline immunodeficiency virus. J. Virol. 76 (23), 11889–11903.

Lever, A., Gottlinger, H., Haseltine, W., Sodroski, J., 1989. Identification of a sequence required for efficient packaging of human immunodeficiency virus type 1 RNA into virions. J. Virol. 63 (9), 4085–4087.

Lever, A.M., Richardson, J.H., Harrison, G.P., 1991. Retroviral RNA packaging. Biochem. Soc. Trans. 19 (4), 963–966.

Linial, M.L., Miller, A.D., 1990. Retroviral RNA packaging: sequence requirements and implications. Curr. Top. Microbiol. Immunol. 157, 125–152.

Loewen, N., Barraza, R., Whitwam, T., Saenz, D., Kemler, I., Poeschla, E., 2003. FIV vectors. Methods Mol. Biol. 229, 251–271.

Luban, J., Goff, S.P., 1991. Binding of human immunodeficiency virus type 1 (HIV-1) RNA to recombinant HIV-1 gag polyprotein. J. Virol. 65 (6), 3203–3212.

Luban, J., Goff, S.P., 1994. Mutational analysis of cis-acting packaging signals in human immunodeficiency virus type 1 RNA. J. Virol. 68 (6), 3784–3793.

McBride, M.S., Panganiban, A.T., 1996. The human immunodeficiency virus type 1 encapsidation site is a multipartite RNA element composed of functional hairpin structures. J. Virol. 70 (5), 2963–2973.

McBride, M.S., Panganiban, A.T., 1997. Position dependence of functional hairpins important for human immunodeficiency virus type 1 RNA encapsidation in vivo. J. Virol. 71 (3), 2050–2058.

McBride, M.S., Schwartz, M.D., Panganiban, A.T., 1997. Efficient encapsidation of human immunodeficiency virus type 1 vectors and further characterization of cis elements required for encapsidation. J. Virol. 71 (6), 4544–4554.

Parolin, C., Dorfman, T., Palu, G., Gottlinger, H., Sodroski, J., 1994. Analysis in human immunodeficiency virus type 1 vectors of cis-acting sequences that affect gene transfer into human lymphocytes. J. Virol. 68 (6), 3888–3895.

Patel, J., Wang, S.W., Izmailova, E., Aldovini, A., 2003. The simian immunodeficiency virus 5′ untranslated leader sequence plays a role in intracellular viral protein accumulation and in RNA packaging. J. Virol. 77 (11), 6284–6292.

Poeschla, E.M., 2003. Non-primate lentiviral vectors. Curr. Opin. Mol. Ther. 5 (5), 529–540.

Poeschla, E., Looney, D., 1998. CXCR4 is required by a non-primate lentivirus: heterologous expression of feline immunodeficiency virus in human, rodent and feline cells. J. Virol. 72 (8), 6858–6866.

Poeschla, E., Gilbert, J., Li, X., Huang, S., Ho, A., Wong-Staal, F., 1998. Identification of a human immunodeficiency virus type 2 (HIV-2) encapsidation determinant and transduction of nondividing human cells by HIV-2-based lentivirus vectors. J. Virol. 72 (8), 6527–6536.

Russell, R.S., Hu, J., Beriault, V., Mouland, A.J., Kleiman, L., Wainberg, M.A., Liang, C., 2003. Sequences downstream of the 5′ splice donor site are required for both packaging and dimerization of human immunodeficiency virus type 1 RNA. J. Virol. 77 (1), 84–96.

Sakalian, M., Hunter, E., 1998. Molecular events in the assembly of retrovirus particles. Adv. Exp. Med. Biol. 440, 329–339.

Strappe, P.M., Greatorex, J., Thomas, J., Biswas, P., McCann, E., Lever, A.M., 2003. The packaging signal of simian immunodeficiency virus is upstream of the major splice donor at a distance from the RNA cap site similar to that of human immunodeficiency virus types 1 and 2. J. Gen. Virol. 84 (Pt 9), 2423–2430.

Sundquist, W.I., Heaphy, S., 1993. Evidence for interstrand quadruplex formation in the dimerization of human immunodeficiency virus 1 genomic RNA [see comments]. Proc. Natl. Acad. Sci. U.S.A. 90 (8), 3393–3397.

Swanstrom, R., Wills, J., 1997. Synthesis, assembly, and processing of viral proteins. In: Coffin, J., Huges, S., Varmus, H. (Eds.), Retroviruses. Cold Spring Harbor Laboratory Press, Cold Spring Harbor, NY, pp. 263–334.

Talbott, R.L., Sparger, E.E., Lovelace, K.M., Fitch, W.M., Pedersen, N.C., Luciw, P.A., Elder, J.H., 1989. Nucleotide sequence and genomic organization of feline immunodeficiency virus. Proc. Natl. Acad. Sci. U.S.A. 86 (15), 5743–5747.

Vicenzi, E., Dimitrov, D.S., Engelman, A., Migone, T.S., Purcell, D.F., Leonard, J., Englund, G., Martin, M.A., 1994. An integration-defective U5 deletion mutant of human immunodeficiency virus type 1 reverts by eliminating additional long terminal repeat sequences. J. Virol. 68 (12), 7879–7890.

Whitwam, T., Peretz, M., Poeschla, E.M., 2001. Identification of a central DNA flap in feline immunodeficiency virus. J. Virol. 75 (19), 9407–9414.